

# Capacity Region Bounds for the $K$ -user Dispersive Nonlinear Optical WDM Channel with Peak Power Constraints

Viswanathan Ramachandran, Gabriele Liga, Astrid Barreiro, and Alex Alvarado  
Eindhoven University of Technology, 5600 MB Eindhoven, the Netherlands

**Abstract**—It is known that fiber nonlinearities induce crosstalk in a wavelength division multiplexed (WDM) system, which limits the capacity of such systems especially at higher signal powers. Traditionally, the channel capacity of a single WDM user is analyzed under different assumptions for the transmitted signals of the other users. In this paper, we instead take a multi-user information theoretic view of an optical WDM channel impaired by cross-phase modulation and dispersion as an interference channel. We characterize, for the first time, an outer bound on the capacity region of simultaneously achievable rate pairs, assuming a general  $K$ -user perturbative channel model using genie-aided techniques. Furthermore, an achievable rate region is obtained by time-sharing between certain single-user strategies, and it is shown that the latter can achieve better rate tuples compared to treating nonlinear interference as noise.

## I. INTRODUCTION

In wavelength division multiplexing (WDM), independent data from different users across different wavelengths are multiplexed into a single optical fiber using several transmitters, with corresponding demultiplexing at the receiver side. The nonlinear Kerr effect in an optical fiber causes the signal in one wavelength to interfere with the signals in other wavelengths. A key feature of interchannel nonlinearity is that the data across all WDM users contribute to the interference impinging on each WDM user, and hence its statistical properties depend on the joint statistics of the transmitted data across all WDM users. One such interchannel nonlinear effect is cross-phase modulation (XPM), where the phase of the signal on the channel of interest is distorted as a function of the intensities of the signals at other wavelengths. It is very difficult to compensate for effects like XPM, since it entails joint detection of multiple channels that is prohibitively complex. The combination of interchannel effects with chromatic dispersion (group velocity dispersion) and noise, result in a stochastic nonlinear channel with memory. Such a channel is described by the (noisy) nonlinear Schrödinger equation (NLSE) (or the Manakov equation in case of dual polarization systems), which considers self-phase modulation (SPM), cross-phase modulation (XPM) and four-wave mixing (FWM). Many modern systems are dominated by XPM, which is often treated by the optical receivers as noise.

The fundamental limits of communication over the NLSE channel fall within the domain of *multiuser information theory*, which investigates trade-offs between the rates at which *all different users* can jointly operate. Unlike single-user information theory, the central object of interest in multiuser

information theory is the capacity *region*, i.e., the region of all simultaneously achievable rates.

The dominant paradigm in optical multi-user channels so far has been the study of achievable rates for individual users in the system. For instance, Secondini and Forestieri [1] studied the capacity of a single user in a WDM system and proved that it grows unbounded with power as opposed to Gaussian achievable information rates that exhibit a finite maximum. Agrell and Karlsson [2] studied the impact of different behavioral models for the interfering users on the capacity of a specific user in the system. These works attempt to reduce the analysis of a multi-user problem to more familiar single-user problems. Moreover, as far as capacity upper bounds are concerned, the only known ones for a general NLSE (single-user waveform) channel are that of Yousefi *et al.* [3], Kramer *et al.* [4] and Keykhosravi *et al.* [5].

In the multi-user information theory literature, multiple one-to-one communications over a shared medium with crosstalk between the users is known as an *interference channel* [6, Chapter 6]. Optical interference channels have attracted very little attention. Only two papers exist in the literature till date, to the best of our knowledge. The earliest such work from 2006 was by Taghavi *et al.* [7], where the benefits of multi-user detection in WDM systems were analyzed by modelling it as a *multiple access channel* (which is nothing but an interference channel with full receiver cooperation). More than ten years later, Ghozlan and Kramer [8] studied a simplified interference channel model based on logarithmic perturbation ignoring group velocity dispersion across WDM bands and introduced the technique of *interference focusing* to achieve the optimal high power pre-log factors.

With the aforementioned exceptions [7], [8], a study of the set of *simultaneously achievable* rates that captures the contention amongst the different users accessing the optical channel transmission resources based on a realistic channel model is not available in the literature. Moreover, capacity upper bounds are as of today also completely missing in the framework of optical multi-user channels.

In this paper, we take a step in this direction and consider a realistic first-order perturbative multi-user model that considers both chromatic dispersion and Kerr nonlinearity. The main contributions of this paper are twofold.

- Firstly, we propose a novel outer bound on the capacity region of a multi-user/WDM channel where both the

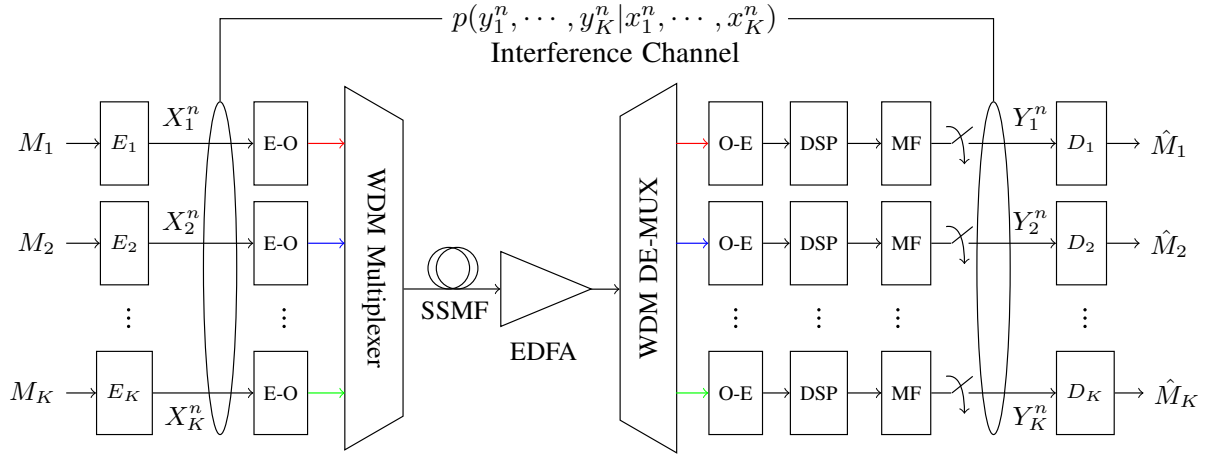


Fig. 1: Interference channel model for WDM transmission.

transmitters and the receivers are independently operated (as is the case with most practical systems).

- Moreover, we obtain an achievable rate region by time-sharing between certain single-user strategies, and show that the latter can achieve better rate tuples than the conventional strategy where optical receivers treat interference arising from other WDM users as noise (abbreviated *TIN* henceforth).

The investigated channel is a first-order perturbative multi-user model where both chromatic dispersion and Kerr nonlinearity are assumed to take effect during fiber propagation. Results in the literature have shown that this model is valid for a wide range of powers and system configurations.

*Paper Organization:* The channel model is first described in Section II. Section III-A describes a baseline achievable region obtained by treating interference as noise. Capacity region outer bounds are derived in Section III-B. Achievable rates for the individual users are computed in Section III-C under constant-amplitude signalling for the interferers. Section III-D contains the numerical results and discussions. Finally, Section IV concludes the paper.

*Notation convention:* Random variables or random vectors are represented by upper-case letters, whereas their realizations are represented by the corresponding lower case characters. All logarithms in this paper are assumed to be with respect to base 2, unless stated otherwise. Given a complex random variable  $X$ , we will denote its real part by  $X^R$  and its imaginary part by  $X^I$ , i.e.,  $X = X^R + jX^I$  with  $j = \sqrt{-1}$ . Also, a length- $n$  block of random symbols is denoted by  $X_k^n \triangleq (X_k[1], X_k[2], \dots, X_k[n])$ , where the subscript  $k$  is a user index and the number within square brackets is a discrete time index.

## II. CHANNEL MODEL

We study the  $K$ -user WDM system shown in Fig. 1, where the interference channel  $p(y_1^n, \dots, y_K^n | x_1^n, \dots, x_K^n)$  encompasses the electro-optical (E-O) conversion, WDM multiplexing, the physical channel composed of  $K$  WDM users and the

optical fiber along with optical amplifier, WDM demultiplexing, optical-electrical (O-E) conversion, dispersion compensation, digital backpropagation, matched filtering and symbol-rate sampling. Given that this is the first study on capacity regions for regular perturbative models, we ignore signal-noise interactions and assume single-polarization transmission over a single span of standard single mode fiber (SSMF).

For such a single-mode fiber with Kerr nonlinearity and chromatic dispersion, the complex envelope of the optical field,  $A(t, z)$ , at time  $t$  and distance  $z$  from the transmitter is governed by the nonlinear Schrödinger equation [9]

$$\frac{\partial A(t, z)}{\partial z} = -\frac{\alpha}{2}A(t, z) + \frac{j}{2}\beta_2 \frac{\partial^2 A(t, z)}{\partial \tau^2} - j\gamma|A(t, z)|^2 A(t, z), \quad (1)$$

where  $\tau = t - \beta_1 z$  is the shifted time reference of the moving pulse. In this expression,  $\alpha$  stands for the fiber attenuation factor,  $\beta_1$  is the inverse of the group velocity,  $\beta_2$  stands for the group velocity dispersion parameter, while  $\gamma$  is the fiber nonlinearity parameter, with the last term on the right-hand side representing Kerr nonlinearity.

The output at the receiver of user- $k$ ,  $k \in \{1, 2, \dots, K\}$ , can be expressed using a first-order regular perturbative discrete-time model [10, eqs. (59),(60)], [11, eqs. (5),(7)]

$$\begin{aligned} Y_k[i] &= X_k[i] + N_k[i] \\ &+ j\gamma \sum_{t=-\infty}^{\infty} X_k[i-t] \\ &\times \sum_{l=-\infty}^{\infty} \sum_{m=-\infty}^{\infty} S_k^{l,m,t} \sum_{\substack{w=1 \\ w \neq k}}^K X_w[i-l] X_w[i-m]^*, \end{aligned} \quad (2)$$

where  $X_k[i]$  represents the input of user- $k$  at time instant  $i \in \{1, 2, \dots, n\}$ ,  $X_w[i]$  for  $w \neq k$  are the inputs of the interfering users at instant  $i$ ,  $X_w[i-l]$  represents the corresponding input at a time lag of  $l$ , and  $\gamma$  is the fiber nonlinearity parameter from (1). The complex channel coefficients  $S_k^{l,m,t}$  are given in [11, eq. (7)], are computed numerically, and depend on the

properties of the optical link and the transmission parameters. In (2),  $N_k[i]$  models amplified spontaneous emission (ASE) noise from the erbium-doped amplifiers (EDFAs). The ASE noise is assumed to be circularly symmetric complex Gaussian with mean zero and variance  $\sigma_k^2$  per complex dimension. We assume length- $n$  codewords with maximum power constraints:

$$\max_{i \in \{1, 2, \dots, n\}} |x_k[i]|^2 \leq P_k, \forall k \in \{1, 2, \dots, K\}, \quad (3)$$

In other words,  $P_k$  represents a peak power constraint on the symbols transmitted by user- $k$ .

Though we assume that self-phase modulation (SPM) is ideally compensated in (2), the results in this paper can be generalized to take into account both SPM as well as XPM. Moreover, we note that the channel model specified by (2) is more realistic compared to the four-wave mixing (FWM) only model studied in Agrell and Karlsson [2], which assumes that both the dispersion and the nonlinearity are weak, and the generalized phase-matching condition is fulfilled [12].

**Example 1** (3 WDM channels). *For the case of  $K = 3$  users, the received symbols for the center channel (user 2) is given by the expression*

$$\begin{aligned} Y_2[i] &= X_2[i] + N_2[i] \\ &+ j\gamma \sum_{t=-\infty}^{\infty} X_2[i-t] \\ &\quad \times \sum_{l=-\infty}^{\infty} \sum_{m=-\infty}^{\infty} S_2^{l,m,t} X_1[i-l] X_1[i-m]^* \\ &+ j\gamma \sum_{t=-\infty}^{\infty} X_2[i-t] \\ &\quad \times \sum_{l=-\infty}^{\infty} \sum_{m=-\infty}^{\infty} S_2^{l,m,t} X_3[i-l] X_3[i-m]^*. \end{aligned} \quad (4)$$

□

It is known from [13, Figs. 4 and 5] and [11, eq. (8)] that for few-span systems of relatively short lengths using lumped amplification, the largest contribution to the nonlinear interference (NLI) comes from the  $S_k^{m,m,0}$  terms in equation (2), i.e., when only two time shifted sequences interact with each other – this corresponds to  $t = 0$  and  $l = m$  in (2).

Furthermore, since physical channels do not have infinite memory, we truncate the sum in (2) to the finite interval  $(-M, M)$  to obtain the following approximate model:

$$\begin{aligned} Y_k[i] &\approx X_k[i] + N_k[i] \\ &+ j\gamma X_k[i] \sum_{m=-M}^M S_k^{m,m,0} \sum_{\substack{w=1 \\ w \neq k}}^K |X_w[i-m]|^2 \\ &\triangleq X_k[i] \left( 1 + j \sum_{m=-M}^M c_k^m \sum_{\substack{w=1 \\ w \neq k}}^K |X_w[i-m]|^2 \right) + N_k[i], \end{aligned} \quad (5)$$

where we have defined

$$\gamma S_k^{m,m,0} \triangleq c_k^m \quad (6)$$

for compactness. Notice that only  $M$  symbols before and after the current time instant contribute to the nonlinear interference, as opposed to the infinite summations involved in (2). We shall work with the model in (5) in the sequel.

### III. MAIN RESULTS

The main results in this paper are organized into four subsections. Firstly, section III-A describes a commonly used scheme in optical systems – that of treating interference arising from other WDM users as noise. This results in an achievable region (inner bound on the capacity region) which we refer to as the TIN region. One of our key contributions, a novel outer bound on the capacity region, is then discussed in section III-B. Next, section III-C describes another inner bound on the capacity region based on time-sharing between certain single-user strategies. Finally, section III-D contains the numerical results and discussions on the performance of these capacity bounds.

#### A. Treating Interference as Noise

In this section, we discuss a simple strategy to obtain an achievable region for the channel model under consideration. Firstly, for all  $k \in \{1, 2, \dots, K\}$ , we choose the inputs  $X_k^n$  to be i.i.d. according to  $p_{X_k}(x_k)$ , where the phase of  $X_k$  is uniform on  $[-\pi, \pi]$  and independent of its amplitude  $|X_k| = R$  that has probability density function:

$$p_R(r) = \begin{cases} \frac{2r}{P_k}, & 0 \leq r \leq \sqrt{P_k} \\ 0, & \text{elsewhere.} \end{cases}$$

We then resort to the most commonly used approach in optical multi-user systems, that involves each user treating nonlinear interference as Gaussian noise. In the context of expression (5), this can be expressed as

$$\begin{aligned} Y_k[i] &= X_k[i] \\ &+ \underbrace{N_k[i] + jX_k[i] \sum_{m=-M}^M c_k^m \sum_{\substack{w=1 \\ w \neq k}}^K |X_w[i-m]|^2}_{\text{noise}}, \end{aligned} \quad (7)$$

wherein the entire term representing the nonlinear interference (NLI) is treated as Gaussian noise with the corresponding variance (evaluated numerically). This will serve as a baseline to compare with the outer and inner bounds to be discussed in the ensuing sections.

#### B. Capacity Region Outer Bounds

In this section, we analyze the region of simultaneously achievable rate pairs  $(R_1, R_2, \dots, R_K)$  for the  $K$ -user model in Fig. 1, modeled by (5). Before stating the outer bound, we need some definitions. An  $(n, 2^{nR_1}, 2^{nR_2}, \dots, 2^{nR_K})$  code for this channel consists of  $K$  message sets  $\{1, 2, \dots, 2^{nR_k}\}$  for  $k \in \{1, 2, \dots, K\}$ ,  $K$  encoders where  $E_k$  maps a message

TABLE I: Model Parameters

Parameter	Value
Memory Length $M$ (eq. (5))	5
Number of WDM users	3
Distance	250 km
Nonlinearity parameter $\gamma$	$1.2 \text{ W}^{-1}\text{km}^{-1}$
Signalling Rate	32 Gbaud
Fiber attenuation $\alpha$	0.2 dB/km
Group velocity dispersion $\beta_2$	$-21.7 \text{ ps}^2/\text{km}$
RRC pulse-shaping roll-off	0.1

$M_k \in \{1, 2, \dots, 2^{nR_k}\}$  into a codeword  $X_k^n(M_k)$ , and  $K$  decoders where  $D_k$  assigns an estimate  $\hat{M}_k$  (or an error message) to each received sequence  $Y_k^n$ . The messages  $M_k$  are assumed to be uniformly drawn on their respective alphabets  $\{1, 2, \dots, 2^{nR_k}\}$  for all  $k \in \{1, 2, \dots, K\}$ . The probability of error is defined as

$$P_e \triangleq \Pr((\hat{M}_1(Y_1^n), \dots, \hat{M}_K(Y_K^n)) \neq (M_1, \dots, M_K)). \quad (8)$$

A rate tuple  $(R_1, R_2, \dots, R_K)$  is said to be *achievable* if there exists a sequence of  $(n, 2^{nR_1}, 2^{nR_2}, \dots, 2^{nR_K})$  codes such that  $\lim_{n \rightarrow \infty} P_e = 0$ . The capacity region  $\mathcal{C}_K$  is the closure of the set of achievable rate tuples  $(R_1, R_2, \dots, R_K)$ .

We now obtain an outer bound on the capacity region  $\mathcal{C}_K$  using genie-aided techniques [14]. The outer bound is stated in the following theorem.

**Theorem 1.** *The capacity region  $\mathcal{C}_K$  of the interference channel in (5) is contained in the region specified by the set of  $(R_1, R_2, \dots, R_K)$  tuples such that*

$$R_k \leq C_k, \forall k \in \{1, 2, \dots, K\}, \quad (9)$$

where

$$C_k \triangleq \log \left( 1 + \frac{P_k}{2\sigma_k^2} \left( 1 + \left( \sum_{\substack{w=1 \\ w \neq k}}^K P_w \sum_{m=-M}^M |c_k^m| \right)^2 \right) \right), \quad (10)$$

and  $c_k^m$  is given in (6).

*Proof.* See Appendix A.  $\square$

In particular, Theorem 1 above also serves to identify the optimal interferer transmissions of users  $w \neq k$  with regards to maximizing the rate of user- $k$ , in addition to defining a fundamental limit on the rates achievable by user- $k$ . This motivates the next section, where achievability strategies are discussed for the different users.

### C. Achievable rates

Consider the channel output for user- $k$ ,  $k \in \{1, 2, \dots, K\}$  in (5). Suppose the interferer transmissions are chosen to be as follows:

$$|x_w[i-m]|^2 = P_w, \forall w \neq k, \text{ and } \forall m \text{ and } \forall i > m. \quad (11)$$

In other words, we use constant amplitude signaling for the interferers. It will be clear from expression (23) (in the proof

of Theorem 1 in Appendix A) that this is indeed the best strategy for maximizing the rate of user- $k$ . Hence we obtain the following memoryless single-user channel (dropping the time indices for simplicity):

$$Y_k = X_k \left( 1 + j \sum_{m=-M}^M c_k^m \sum_{\substack{w=1 \\ w \neq k}}^K P_w \right) + N_k. \quad (12)$$

Notice that (12) is a complex AWGN channel with a peak power constraint on the input  $X_k$ , which has been extensively studied in the information theory literature [15], [16], [17], [18], [19]. It is known that the capacity achieving input distribution for this channel is discrete in amplitude with uniform phase. No closed form expressions exist for the capacity of the channel, but the number of mass points for the amplitude of the capacity achieving input distribution as a function of the peak signal to noise ratio have been characterized [16].

For our purposes of computing an achievable rate for user- $k$  in (12) under constant amplitude signaling for the interferers, we resort to the lower bounding technique used in [16, Equation (38)], based on the entropy power inequality. We have the following theorem that concerns achievable rates for user- $k$ ,  $k \in \{1, 2, \dots, K\}$ .

**Theorem 2.** *The capacity of the memoryless single-user channel from  $X_k$  to  $Y_k$ ,  $k \in \{1, 2, \dots, K\}$  in (12) is lower bounded as:*

$$\tilde{C}_k \geq \log \left( 1 + \frac{P_k}{2\sigma_k^2 e} \left( 1 + \left( \sum_{\substack{w=1 \\ w \neq k}}^K P_w \sum_{m=-M}^M |c_k^m| \right)^2 \right) \right). \quad (13)$$

This defines an achievable rate for user- $k$  in the model specified by (5) under constant amplitude signaling for the interferers (all users  $w \neq k$ ).

*Proof.* See Appendix B.  $\square$

The strategy of constant amplitude signaling for the interferers  $w \neq k$ , along with the scheme used to achieve the right-hand side of (13) in Theorem 2 (see Appendix B for the details) for user- $k$ ,  $k \in \{1, 2, \dots, K\}$ , together define  $K$  achievable rate tuples on the  $K$ -dimensional plane. Time-sharing between such achievable rate tuples yields another inner bound for the channel in (5). A comparison between the TIN inner bound, the outer bound in Theorem 1 and the inner bound obtained by time-sharing between rate tuples resulting from Theorem 2 follow in the next section.

### D. Numerical Results

The parameters used in our numerical results are summarized in Table I. As in Example 1, we consider the case of  $K = 3$  WDM channels. We have taken  $M = 5$  in (5) since this is a good approximation to the channel memory for a single-span system of length 250 km.

The genie-aided outer bound on user-1 ( $C_1$ ) in Theorem 1 and the corresponding lower bound  $\tilde{C}_1$  in Theorem 2 are plotted in Fig. 2 against the peak input power

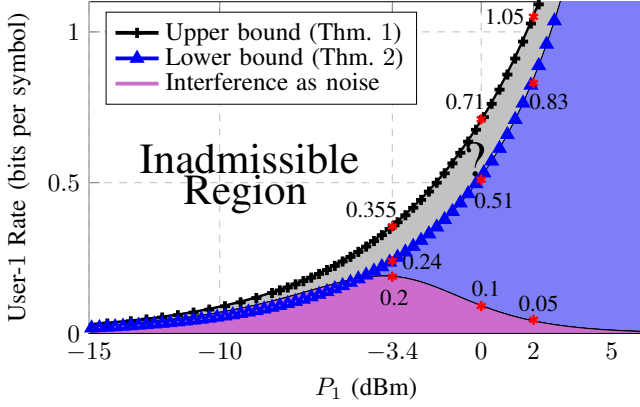


Fig. 2: Outer bound in Theorem 1, achievable rate in Theorem 2 and the baseline scheme of treating interference as noise versus peak input power. The points marked in red correspond to peak input powers of  $-3.4$  dBm,  $0$  dBm, and  $2$  dBm, with the values of the  $y$ -coordinates on the corresponding capacity curves marked alongside. These values will be used in the three dimensional depiction of the corresponding rate regions in Fig. 3.

for the symmetric case of  $P_1 = P_2 = P_3$ . For comparison, the lower bound obtained by treating the interference term  $jX_k[i] \sum_{m=-M}^M c_k^m \sum_{w \neq k} |X_w[i-m]|^2$  in (5) as Gaussian noise (whose variance is computed numerically) are also shown, by choosing the inputs  $X_k^n$  to be i.i.d. according to the pdf described in Section III-A for all  $k \in \{1, 2, 3\}$ . The shaded areas in purple and blue are achievable, while the area marked ‘inadmissible’ is not achievable as a consequence of Theorem 1. The achievability of the shaded area in gray remains unknown.

In Figs. 3(a) – (c), we plot the trade-off between the rates of the three users for fixed (and equal) powers of  $-3.4$  dBm,  $0$  dBm and  $2$  dBm, respectively (see the red stars in Fig. 2). The cubical region implied by the genie-aided outer bound in Theorem 1 is shown by solid black lines in Figs. 3(a)–(c). For comparison, we have depicted the respective achievable rate regions obtained by treating the interference terms in (5) as Gaussian noise as the cubical regions in purple. Note that these *interference as noise* regions eventually vanish in the highly nonlinear regime.

The strategy of constant amplitude signaling for the interferers (users  $w \neq k$ ) along with Theorem 2 for user- $k$ ,  $k \in \{1, 2, 3\}$ , defines 3 achievable rate triples on the 3-dimensional plane. Time-sharing between these achievable rate triples yields another achievable region for the channel in (5). These polyhedral regions are depicted in blue in Figs. 3(a)–(c). It is observed that the simple strategy of time-sharing between such single-user codes outperforms treating interference as noise. In fact, the relative gains of time-sharing (in terms of better achievable rate tuples) compared to treating interference as noise becomes more pronounced with increasing powers, as can be seen in the evolution from Fig 3(a) to Fig. 3(c).

## IV. CONCLUSIONS

We took a multi-user information theoretic view of a  $K$ -user wavelength division multiplexing system impaired by cross-phase modulation and dispersion, and derived a novel capacity region outer bound using genie-aided techniques. An achievable rate region was also obtained for the same, and it was shown that time-sharing between certain single-user schemes can strictly outperform treating interference as noise. This is the very first step towards a multi-user characterization of fiber optic systems, breaking away from the traditional single-user perspective. Future works include obtaining tighter achievable regions/inner bounds as well as outer bounds, and the design and implementation of schemes that can achieve the presented capacity bounds in practice.

## ACKNOWLEDGEMENTS

The authors would like to thank Hamdi Joudeh for useful discussions. The work of V. Ramachandran, A. Barreiro and A. Alvarado has received funding from the European Research Council (ERC) under the European Union’s Horizon 2020 research and innovation programme (grant agreement No 757791). The work of G. Liga is funded by the EuroTech-Postdoc programme under the European Union’s Horizon 2020 research and innovation programme (Marie Skłodowska-Curie grant agreement No 754462).

## APPENDIX A PROOF OF THEOREM 1

We now establish the outer bound using information theoretic inequalities. The rate of user- $k$ ,  $k \in \{1, 2, \dots, K\}$ , can be upper bounded as follows:

$$\begin{aligned}
nR_k &= H(M_k) \\
&\stackrel{(a)}{=} H(M_k | \{X_w^n | w \neq k\}) \\
&= H(M_k | \{X_w^n | w \neq k\}, Y_k^n) \\
&\quad + H(M_k | \{X_w^n | w \neq k\}, Y_k^n) \\
&\stackrel{(b)}{\leq} I(M_k; Y_k^n | \{X_w^n | w \neq k\}) + H(M_k | Y_k^n) \\
&\stackrel{(c)}{\leq} I(M_k; Y_k^n | \{X_w^n | w \neq k\}) + 1 + P_e nR_k \\
&\stackrel{(d)}{=} I(M_k; Y_k^n | \{X_w^n | w \neq k\}) + n\epsilon_n \\
&\stackrel{(e)}{\leq} I(X_k^n, Y_k^n | \{X_w^n | w \neq k\}) + n\epsilon_n \\
&= h(Y_k^n | \{X_w^n | w \neq k\}) - h(Y_k^n | X_k^n, \{X_w^n | w \neq k\}) + n\epsilon_n \\
&= h(Y_k^n | \{X_w^n | w \neq k\}) - h(N_k^n) + n\epsilon_n \\
&\stackrel{(f)}{\leq} \sum_{i=1}^n h(Y_k[i] | \{X_w^n | w \neq k\}) - \sum_{i=1}^n h(N_k[i]) + n\epsilon_n \\
&\stackrel{(g)}{\leq} \sum_{i=1}^n \max_{\{x_w^n | w \neq k\}} [h(Y_k[i] | \{X_w^n = x_w^n | w \neq k\})] \\
&\quad - \sum_{i=1}^n h(N_k[i]) + n\epsilon_n
\end{aligned}$$

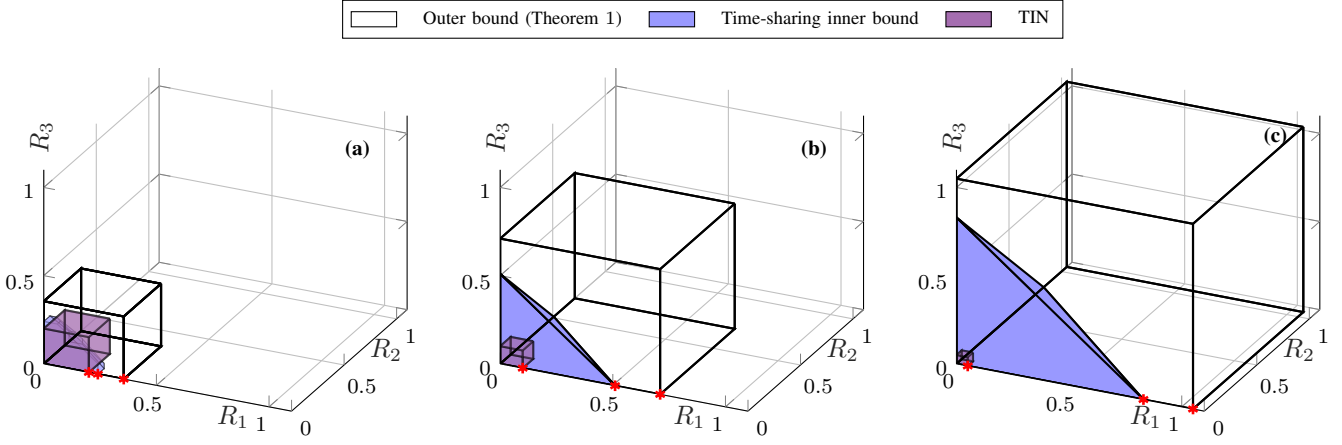


Fig. 3: Outer bound rate region in Theorem 1 and inner bound regions for a peak transmitted power per user of (a)  $-3.4$  dBm, (b)  $0$  dBm, and (c)  $2$  dBm. The intercepts of the different regions on each of the axes correspond to the red starred values in Fig. 2.

$$\stackrel{(h)}{\leq} \sum_{i=1}^n \max_{\{x_w^n | w \neq k\}} \left[ \frac{1}{2} \log \left( \frac{\det \left( \text{cov} \left( Y_k[i]^R, Y_k[i]^I \mid \{X_w^n = x_w^n | w \neq k\} \right) \right)}{(\sigma_k^2)^2} \right) \right] + n\epsilon_n, \quad (14)$$

where (a) follows since  $M_k$  is independent of  $\{X_w^n | w \neq k\}$ , (b) follows since conditioning does not increase the entropy, (c) follows from Fano's inequality with  $P_e$  being defined as in (8), (d) follows by defining  $\epsilon_n = (1/n + P_e R_k)$  with  $\epsilon_n \xrightarrow{n \rightarrow \infty} 0$ , (e) follows from the data processing inequality since  $M_k \rightarrow X_k^n \rightarrow Y_k^n$  form a Markov chain in that order conditioned on  $\{X_w^n | w \neq k\}$ , (f) follows since conditioning does not increase the entropy and the fact that the additive noise is i.i.d., (g) follows since  $h(Y_k[i] | \{X_w^n | w \neq k\})$  represents an average over  $\{x_w^n | w \neq k\}$  and the average is upper bounded by the maximum, while (h) follows from the fact that Gaussian random vectors maximize the differential entropy under a covariance constraint.

It now remains to bound the  $\log(\det(\cdot))$  terms in expression (14). Equation (5) can be expressed in terms of its respective real and imaginary components. Thus we have

$$Y_k[i]^R = X_k[i]^R - \sum_{\substack{w=1 \\ w \neq k}}^K \sum_{m=-M}^M c_k^m |X_w[i-m]|^2 X_k[i]^I + N_k[i]^R, \quad (15)$$

$$Y_k[i]^I = X_k[i]^I + \sum_{\substack{w=1 \\ w \neq k}}^K \sum_{m=-M}^M c_k^m |X_w[i-m]|^2 X_k[i]^R + N_k[i]^I. \quad (16)$$

Let  $\mathbb{E}[(X_k[i]^R)^2] = p_{k,i}^R$  and  $\mathbb{E}[(X_k[i]^I)^2] = p_{k,i}^I$  such that  $p_{k,i}^R + p_{k,i}^I \leq P_{k,i}$  from the power constraint. Hence we can write the following chain of inequalities for the determinant of the covariance matrix involved in (14):

$$\det(\text{cov}(Y_k[i]^R, Y_k[i]^I | \{X_w^n = x_w^n | w \neq k\}))$$

$$\begin{aligned} &= \det \left( \text{cov} \left( X_k[i]^R \right. \right. \\ &\quad \left. \left. - \sum_{\substack{w=1 \\ w \neq k}}^K \sum_{m=-M}^M c_k^m |X_w[i-m]|^2 X_k[i]^I + N_k[i]^R, \right. \right. \\ &\quad \left. \left. X_k[i]^I \right. \right. \\ &\quad \left. \left. + \sum_{\substack{w=1 \\ w \neq k}}^K \sum_{m=-M}^M c_k^m |X_w[i-m]|^2 X_k[i]^R + N_k[i]^I \right. \right. \\ &\quad \left. \left. \mid \{X_w^n = x_w^n | w \neq k\} \right) \right) \\ &= \det \left( \text{cov} \left( X_k[i]^R \right. \right. \\ &\quad \left. \left. - \sum_{\substack{w=1 \\ w \neq k}}^K \sum_{m=-M}^M c_k^m |x_w[i-m]|^2 X_k[i]^I + N_k[i]^R, \right. \right. \\ &\quad \left. \left. X_k[i]^I \right. \right. \\ &\quad \left. \left. + \sum_{\substack{w=1 \\ w \neq k}}^K \sum_{m=-M}^M c_k^m |x_w[i-m]|^2 X_k[i]^R + N_k[i]^I \right) \right)^2 \\ &\stackrel{(a)}{\leq} \frac{1}{4} \left( \text{var} \left( X_k[i]^R \right. \right. \\ &\quad \left. \left. - \sum_{\substack{w=1 \\ w \neq k}}^K \sum_{m=-M}^M c_k^m |x_w[i-m]|^2 X_k[i]^I + N_k[i]^R \right) \right. \\ &\quad \left. + \text{var} \left( X_k[i]^I \right. \right. \\ &\quad \left. \left. + \sum_{\substack{w=1 \\ w \neq k}}^K \sum_{m=-M}^M c_k^m |x_w[i-m]|^2 X_k[i]^R + N_k[i]^I \right) \right) \end{aligned}$$

$$\begin{aligned}
&= \frac{1}{4} \left( p_{k,i}^R + p_{k,i}^I + 2\sigma_k^2 \right. \\
&\quad \left. + \left( \sum_{\substack{w=1 \\ w \neq k}}^K \sum_{m=-M}^M c_k^m |x_w[i-m]|^2 \right)^2 (p_{k,i}^R + p_{k,i}^I) \right)^2 \\
&\stackrel{(b)}{\leq} \frac{1}{4} \left( P_{k,i} \left( 1 + \left( \sum_{\substack{w=1 \\ w \neq k}}^K \sum_{m=-M}^M c_k^m |x_w[i-m]|^2 \right)^2 \right) + 2\sigma_k^2 \right)^2, \tag{17}
\end{aligned}$$

where (a) follows since  $\det(A) \leq \left(\frac{\text{trace}(A)}{n}\right)^n$  for any  $n \times n$  square matrix  $A$ , while (b) follows from the fact that  $p_{k,i}^R + p_{k,i}^I \leq P_{k,i}$  from the power constraint. From expressions (14) and (17), we obtain the following expression for the rate of user- $k$ ,  $k \in \{1, 2, \dots, K\}$ :

$$\begin{aligned}
&n(R_k - \epsilon_n) \\
&\leq \sum_{i=1}^n \max_{\{x_w^n | w \neq k\}} \\
&\quad \left[ \log \left( 1 + \frac{P_{k,i}}{2\sigma_k^2} \left( 1 + \left( \sum_{\substack{w=1 \\ w \neq k}}^K \sum_{m=-M}^M c_k^m |x_w[i-m]|^2 \right)^2 \right) \right) \right]. \tag{18}
\end{aligned}$$

It now remains to solve the optimization problem involved in expression (18) for the optimal interferer realizations. Since  $\log(\cdot)$  is a monotone function, we are interested in the following optimization:

$$M_K = \max_{\substack{\{x_w^n | w \neq k\} \\ \max_m |x_w[m]|^2 \leq P_w \forall w \neq k}} \sum_{\substack{w=1 \\ w \neq k}}^K \sum_{m=-M}^M c_k^m |x_w[i-m]|^2. \tag{19}$$

Notice that the objective function  $\sum_{\substack{w=1 \\ w \neq k}}^K \sum_{m=-M}^M c_k^m |x_w[i-m]|^2$  consists of a dot product of the channel coefficient vector and the vector comprising the squared absolute values of the interferer symbols. Firstly, let us consider the case when the summation index  $m$  in the objective function takes on non-negative values. We perform appropriate zero-padding to make the vector of channel coefficients match the block length  $n$  in size. Then applying Hölder's inequality, we can bound the objective function for each  $w \neq k$  as

$$\begin{aligned}
\sum_{m \geq 0} c_k^m |x_w[i-m]|^2 &\leq \sum_{m \geq 0} |c_k^m |x_w[i-m]|^2| \\
&\leq \left( \max_{m \geq 0} |x_w[i-m]|^2 \right) \left( \sum_{m \geq 0} |c_k^m| \right) \\
&\leq P_w \left( \sum_{m \geq 0} |c_k^m| \right)
\end{aligned}$$

$$= P_w \left( \sum_{m \geq 0} c_k^m \right), \tag{20}$$

where the last step follows since the coefficients  $c_k^m$  (computed along the direction  $t = 0$  and  $l = m$  in (2) using [11, Equation (8)]) are known to be positive.

We next consider the case when the summation index  $m$  in the objective function takes on negative values. The bounding approach here is similar to (20). The objective function for each  $w \neq k$  can be written as

$$\begin{aligned}
\sum_{m < 0} c_k^m |x_w[i-m]|^2 &\stackrel{(a)}{=} \sum_{m' > 0} c_k^{-m'} |x_w[i+m']|^2 \\
&\stackrel{(b)}{=} \sum_{m' > 0} c_k^{m'} |x_w[i+m']|^2 \\
&\leq \sum_{m' > 0} |c_k^{m'} |x_w[i+m']|^2| \\
&\leq \left( \max_{m' > 0} |x_w[i+m']|^2 \right) \left( \sum_{m' > 0} |c_k^{m'}| \right) \\
&\leq P_w \left( \sum_{m' > 0} |c_k^{m'}| \right) \\
&= P_w \left( \sum_{m' > 0} c_k^{m'} \right), \tag{21}
\end{aligned}$$

where (a) follows from a simple change of variables  $m' = -m$  and (b) follows from the symmetry about  $m = 0$  of the coefficients  $c_k^m$  (computed along the direction  $t = 0$  and  $l = m$  in (2) using [11, Equation (8)]). Combining the bounds (20) and (21), we obtain

$$\sum_{m=-M}^M c_k^m |x_w[i-m]|^2 \leq P_w \left( \sum_{m=-M}^M c_k^m \right), \tag{22}$$

Equality holds in (22) with the choice of

$$|x_w[i-m]|^2 = P_w \forall w \neq k, \& \forall m, \& \forall i > m. \tag{23}$$

Using (22), the upper bound in (18) now becomes

$$\begin{aligned}
&n(R_k - \epsilon_n) \\
&\leq \sum_{i=1}^n \left[ \log \left( 1 + \frac{P_{k,i}}{2\sigma_k^2} \left( 1 + \left( \sum_{\substack{w=1 \\ w \neq k}}^K P_w \sum_{m=-M}^M |c_k^m| \right)^2 \right) \right) \right] \\
&\stackrel{(a)}{\leq} n \log \left( 1 + \frac{1}{n} \sum_{i=1}^n \frac{P_{k,i}}{2\sigma_k^2} \left( 1 + \left( \sum_{\substack{w=1 \\ w \neq k}}^K P_w \sum_{m=-M}^M |c_k^m| \right)^2 \right) \right) \\
&\stackrel{(b)}{\leq} n \log \left( 1 + \frac{P_k}{2\sigma_k^2} \left( 1 + \left( \sum_{\substack{w=1 \\ w \neq k}}^K P_w \sum_{m=-M}^M |c_k^m| \right)^2 \right) \right), \tag{24}
\end{aligned}$$

where (a) follows from Jensen's inequality, while (b) follows since the maximum power constraint implies the average power constraint. Dividing throughout by  $n$  and letting  $n \rightarrow \infty$

(which makes  $\epsilon_n \rightarrow 0$ ) completes the proof of the theorem.

## APPENDIX B PROOF OF THEOREM 2

Consider the memoryless single-user channel in (12):

$$Y_k = X_k \left( 1 + j \sum_{m=-M}^M c_k^m \sum_{\substack{w=1 \\ w \neq k}}^K P_w \right) + N_k. \quad (25)$$

The mutual information between  $X_k$  and  $Y_k$  can be bounded as:

$$\begin{aligned} I(X_k; Y_k) &= h(Y_k) - h(Y_k | X_k) \\ &= h(Y_k) - h(N_k) \\ &\stackrel{(a)}{\geq} \ln \left( e^{h \left( X_k \left( 1 + j \sum_{\substack{w=1 \\ w \neq k}}^K P_w \sum_{m=-M}^M c_k^m \right) \right)} + e^{h(N_k)} \right) \\ &\quad - \ln(2\pi e \sigma_k^2) \\ &= \ln \left( e^{h(X_k) + \ln \left( 1 + \left( \sum_{\substack{w=1 \\ w \neq k}}^K P_w \sum_{m=-M}^M |c_k^m| \right)^2 \right)} + 2\pi e \sigma_k^2 \right) \\ &\quad - \ln(2\pi e \sigma_k^2), \end{aligned} \quad (26)$$

where (a) follows from the entropy power inequality. Now we choose the input distribution of  $X_k$  as in [16, Equation (30)] to maximize the differential entropy  $h(X_k)$ , with the phase of  $X_k$  being uniform on  $[-\pi, \pi]$  and independent of the amplitude  $|X_k| = R$  that has probability density function:

$$p_R(r) = \begin{cases} \frac{2r}{P_k}, & 0 \leq r \leq \sqrt{P_k} \\ 0, & \text{elsewhere.} \end{cases}$$

This leads to [16, Equation (37)]

$$h(X_k) = \ln(\pi P_k). \quad (27)$$

Substituting (27) in (26), we obtain

$$\begin{aligned} I(X_k; Y_k) &\geq \ln \left( e^{\ln(\pi P_k) + \ln \left( 1 + \left( \sum_{\substack{w=1 \\ w \neq k}}^K P_w \sum_{m=-M}^M |c_k^m| \right)^2 \right)} + 2\pi e \sigma_k^2 \right) \\ &\quad - \ln(2\pi e \sigma_k^2) \\ &= \ln \left( 1 + \frac{P_k}{2\sigma_k^2 e} \left( 1 + \left( \sum_{\substack{w=1 \\ w \neq k}}^K P_w \sum_{m=-M}^M |c_k^m| \right)^2 \right) \right) \text{ nats} \\ &= \log \left( 1 + \frac{P_k}{2\sigma_k^2 e} \left( 1 + \left( \sum_{\substack{w=1 \\ w \neq k}}^K P_w \sum_{m=-M}^M |c_k^m| \right)^2 \right) \right) \text{ bits.} \end{aligned} \quad (28)$$

This completes the proof.

## REFERENCES

- [1] M. Secondini and E. Forestieri, "Scope and limitations of the nonlinear Shannon limit," *Journal of Lightwave Technology*, vol. 35, no. 4, pp. 893–902, 2016.
- [2] E. Agrell and M. Karlsson, "Influence of behavioral models on multiuser channel capacity," *Journal of Lightwave Technology*, vol. 33, no. 17, pp. 3507–3515, 2015.
- [3] M. I. Yousefi, G. Kramer, and F. R. Kschischang, "Upper bound on the capacity of the nonlinear Schrödinger channel," in *2015 IEEE 14th Canadian Workshop on Information Theory (CWIT)*. IEEE, 2015, pp. 22–26.
- [4] G. Kramer, M. I. Yousefi, and F. R. Kschischang, "Upper bound on the capacity of a cascade of nonlinear and noisy channels," in *2015 IEEE Information Theory Workshop (ITW)*. IEEE, 2015, pp. 1–4.
- [5] K. Keykhosravi, G. Durisi, and E. Agrell, "A tighter upper bound on the capacity of the nondispersive optical fiber channel," in *2017 European Conference on Optical Communication (ECOC)*. IEEE, 2017, pp. 1–3.
- [6] A. El Gamal and Y.-H. Kim, *Network Information Theory*. Cambridge University Press, 2011.
- [7] M. H. Taghavi, G. C. Papan, and P. H. Siegel, "On the multiuser capacity of WDM in a nonlinear optical fiber: Coherent communication," *IEEE Transactions on Information Theory*, vol. 52, no. 11, pp. 5008–5022, 2006.
- [8] H. Ghozlan and G. Kramer, "Models and information rates for multiuser optical fiber channels with nonlinearity and dispersion," *IEEE Transactions on Information Theory*, vol. 63, no. 10, pp. 6440–6456, 2017.
- [9] G. P. Agrawal, "Nonlinear fiber optics." Academic Press, San Diego, 1989.
- [10] A. Mecozzi and R.-J. Essiambre, "Nonlinear Shannon limit in pseudolinear coherent systems," *Journal of Lightwave Technology*, vol. 30, no. 12, pp. 2011–2024, 2012.
- [11] R. Dar, M. Feder, A. Mecozzi, and M. Shtaif, "Properties of nonlinear noise in long, dispersion-uncompensated fiber links," *Optics Express*, vol. 21, no. 22, pp. 25 685–25 699, 2013.
- [12] G. Cappellini and S. Trillo, "Third-order three-wave mixing in single-mode fibers: exact solutions and spatial instability effects," *JOSA B*, vol. 8, no. 4, pp. 824–838, 1991.
- [13] R. Dar, M. Feder, A. Mecozzi, and M. Shtaif, "Pulse collision picture of inter-channel nonlinear interference in fiber-optic communications," *Journal of Lightwave Technology*, vol. 34, no. 2, pp. 593–607, 2016.
- [14] R. H. Etkin, D. N. C. Tse, and H. Wang, "Gaussian interference channel capacity to within one bit," *IEEE Transactions on Information Theory*, vol. 54, no. 12, pp. 5534–5562, 2008.
- [15] J. G. Smith, "The information capacity of amplitude-and variance-constrained scalar gaussian channels," *Information and control*, vol. 18, no. 3, pp. 203–219, 1971.
- [16] S. Shamai and I. Bar-David, "The capacity of average and peak-power-limited quadrature gaussian channels," *IEEE Transactions on Information Theory*, vol. 41, no. 4, pp. 1060–1071, 1995.
- [17] N. Sharma and S. Shamai, "Transition points in the capacity-achieving distribution for the peak-power limited awgn and free-space optical intensity channels," *Problems of Information Transmission*, vol. 46, no. 4, pp. 283–299, 2010.
- [18] A. Thangaraj, G. Kramer, and G. Böcherer, "Capacity bounds for discrete-time, amplitude-constrained, additive white gaussian noise channels," *IEEE Transactions on Information Theory*, vol. 63, no. 7, pp. 4172–4182, 2017.
- [19] A. Dytso, S. Yagli, H. V. Poor, and S. S. Shitz, "The capacity achieving distribution for the amplitude constrained additive gaussian channel: An upper bound on the number of mass points," *IEEE Transactions on Information Theory*, vol. 66, no. 4, pp. 2006–2022, 2019.